This article has been accepted for publication in a future issue of this journal, but has not been fully edited. Content may change prior to final publication. Citation information: DOI10.1109/TFUZZ.2023.3282044, IEEE Transactions on Fuzzy Systems

Ultimately Bounded PID Control For T-S Fuzzy Systems Under FlexRay Communication Protocol

Yezheng Wang, Zidong Wang, Lei Zou, Lifeng Ma, and Hongli Dong

***Abstract*—This paper investigates the ultimately bounded proportional-integral-derivative (PID) control problem for a class of discrete-time Takagi-Sugeno fuzzy systems subject to unknown-but-bounded noises and protocol constraints. The signal transmissions from sensors to the remote controller are realized via a communication network, where the FlexRay protocol is employed to flexibly schedule the information exchange. Such FlexRay protocol is characterized by both the time- and event-triggered mechanisms which are conducted in a cyclic manner. By using a piecewise approach, the measurement outputs affected by the FlexRay protocol are established based on a switching model. Then, a fuzzy PID controller is proposed with a concise and realizable structure. To evaluate the performance of the controlled system, a special time-sequence is introduced that accounts for the behavior of the FlexRay protocol. Subsequently, a general framework is obtained to verify the boundedness of the closed-loop system and then the controller gains are designed by minimizing the bound of the concerned variables. In the end, a simulation study is conducted to validate the effectiveness of the developed control scheme.**

***Index Terms*—Fuzzy systems, proportional-integral-derivative control, FlexRay communication protocol, ultimately bounded control, networked control systems.**

I. Introduction

Networked control systems (NCSs) have now become increasingly popular in engineering practice. Unlike traditional point-to-point systems that use wire-based transmission mechanisms, NCSs connect their components through shared communication networks to exchange information [1]–[8]. The utilization of these networks allows for remote signal transmissions with low cost, feasible operation, and simple maintenance, leading to successful applications of NCSs in various fields such as regional exploration, smart homes, and driverless cars [9]–[13]. Over the past few decades, many researchers have devoted their attention to NCSs with focus on remote control, filtering, and fault diagnosis issues [14]–[21].

With the increase of the system scale, fundamental concern has been raised regarding restrained network resources (i.e., the limited bandwidth) because overloaded data transmissions can cause congestion and further give rise to network-induced phenomena (such as packet dropouts and time delays), which pose threats to the system stability. To address such concern, communication protocols are often employed in the industry to schedule network resources at the cost of sacrificing certain system performance [22], [23]. The commonly used protocols, which tackle network traffic according to different scheduling principles, include the try-once-discard protocol (TODP) [24], Round-Robin protocol (RRP) [25], and stochastic communication protocol [26]. Specifically speaking, the TODP is an event-based protocol that gives system node rights to access networks based on a dynamic competition-based principle. The RRP is a time-triggered protocol that selects system nodes in terms of a fixed circular order. The SCP chooses nodes randomly under some probability constraints. It should be noted that the employed protocols change the traditional signal transmission process and have great effects on NCSs, which have aroused a rich body of research interests [19], [27]–[31].

In addition to the above-mentioned three protocols, special attention has been recently given to the so-called FlexRay protocol (FRP) owing to its prominent flexibility and reliability. The FRP is essentially a hybrid protocol that orchestrates network resources in terms of preset communication cycles composed of static segments and dynamic segments. In the static segment, some time-triggered rules are activated to deal with data packets with a high real-time requirement. When the dynamic segment is encountered, some event-triggered rules are carried out based on data priority. Such features achieve a desired network transmission performance and have contributed to broad applications of the FRP [32]. Within the academic communities, some seminal results have been reported on control/filtering issues of NCSs with the FRPs, see e.g., [33]–[37]. It is worth mentioning that most relevant literature has focused on continuous-time systems, and few results have dealt with discrete-time linear systems. Nevertheless, the corresponding control problem for nonlinear NCSs with FRPs has not drawn enough attention.

This work was supported in part by the National Natural Science Foundation of China under Grants 61933007, 62273087, 62273180, U21A2019, and 62233012, the Shanghai Pujiang Program of China under Grant 22PJ1400400, the Hainan Province Science and Technology Special Fund of China under Grant ZDYF2022SHFZ105, the Royal Society of the UK, and the Alexander von Humboldt Foundation of Germany. *(Corresponding author: Zidong Wang.)*

Yezheng Wang is with the College of Electrical Engineering and Automation, Shandong University of Science and Technology, Qingdao 266590, China. (Email: wangyz_sdust@163.com).

Zidong Wang is with the College of Electrical Engineering and Automation, Shandong University of Science and Technology, Qingdao 266590, China; and is also with the Department of Computer Science, Brunel University London, Uxbridge, Middlesex, UB8 3PH, United Kingdom. (Email: Zidong.Wang@brunel.ac.uk).

Lei Zou is with the College of Information Science and Technology, Donghua University, Shanghai 201620, China; and is also with the Engineering Research Center of Digitalized Textile and Fashion Technology, Ministry of Education, Shanghai 201620, China. (Email: zouleicup@gmail.com).

Lifeng Ma is with the School of Automation, Nanjing University of Science and Technology, Nanjing 210094, China. (Email: malifeng@njust.edu.cn).

Hongli Dong is with the Sanya Offshore Oil and Gas Research Institute, Northeast Petroleum University, Sanya 572025, China; is also with the Artificial Intelligence Energy Research Institute, Northeast Petroleum University, Daqing 163318, China; and is also with the Heilongjiang Provincial Key Laboratory of Networking and Intelligent Control, Northeast Petroleum University, Daqing 163318, China. (Email: shiningdhl@vip.126.com).

It is well known that nonlinearity exists widely in reality, and the investigation on nonlinear NCSs has gradually become a research hotspot in system science. Through a literature review, it can be concluded that the methods of analyzing nonlinear NCSs mainly include assumption (on nonlinearities) based approaches [38], Takagi-Sugeno (T-S) fuzzy control approaches [39], [40], adaptive control methods [41], and linear-parameter-varying model approaches [42]. Among these methods, the T-S fuzzy control is known for the desired approximation capability of nonlinearity and the concise structure of the T-S fuzzy model, thereby attracting extensive research attention in the past decades [43].

The main idea of T-S fuzzy control is to describe a nonlinear plant via the T-S fuzzy model with linear submodels connected by nonlinearity-dependent membership functions [44]. Then, fuzzy controllers are designed according to some specific performance requirements. Typical fuzzy controllers include fuzzy state-feedback controllers [45], [46], fuzzy output-feedback controllers [47], [48], fuzzy sliding-mode controllers [49], fuzzy proportional-integral-derivative (PID) controllers, and fuzzy observer-based controllers [50]. In particular, a general event-triggering communication scheme was proposed, for the first time, in [47] for facilitating the establishment of an elegant T-S fuzzy control framework through co-designing the fuzzy controller gain and the event-triggering threshold, thereby making fundamental contributions to the fuzzy control area. The fuzzy PID controller stands out because of its robustness and prominent control performance. A fuzzy PID controller can be regarded as a combination of several linear PID ones with designed weights and thus enjoys advantages of both fuzzy control and PID control [51]. Many kinds of systems have been considered for the fuzzy PID control problems, and some representative works have been published [52]–[54].

Regarding the existing works relevant to NCSs with the FRP, the following observations have been made: 1) most results have been obtained for continuous-time systems with or without external noises [34]–[36]; and 2) few results have been concerned with linear discrete-time systems subject to bounded noises, and the corresponding results are thus inapplicable to general nonlinear systems [33], [37]. In view of these observations, it is concluded that the fuzzy PID control problem has not received enough attention yet for discrete-time nonlinear NCSs with unknown-but-bounded (UBB) noises and the FRPs. In fact, the existing methods tackling the FRP (such as the lifting method [33]) are no longer applicable to the fuzzy control strategy due to the lack of considering effects of membership functions. Thus, the main motivation is to narrow such a gap.

Summarizing the discussions made so far, studying the fuzzy PID control problem for nonlinear NCSs with FRPs and UBB noises is of both theoretical significance and practical importance. In doing so, the challenges faced are identified as follows: 1) how to construct an appropriate transmission model to reflect the FRP effects under the fuzzy control framework? 2) how to analyze the performance of the closed-loop system with noises and FRP constraints? and 3) how to design the PID controller such that the controlled fuzzy system is ultimately bounded in the presence of the UBB noises? Corresponding to these difficulties, the main contributions of this paper are highlighted as follows: 1) for the first time, the fuzzy PID control issue is investigated for nonlinear NCSs with FRPs and UBB noises; 2) a novel model is proposed to characterize the transmitted measurements affected by FRPs, which is beneficial for the fuzzy controller to be implemented; and 3) the desired gains of the fuzzy PID controller are derived via feasible computational algorithms.

The remainder of this paper is organized as follows. In Section II, the considered fuzzy model, the FRP, the proposed fuzzy PID controller, and the prescribed performance requirement are introduced. Section III analyzes the boundedness of the controlled system and provides results of calculating controller parameters. Section IV presents a simulation example to verify the usefulness of the proposed fuzzy control scheme. Finally, in Section V, the conclusion of this paper is drawn.

Notations: In this paper, $\mathbb{R}^n$ denotes n-dimensional Euclidean space. $\mathbb{N}$ stands for the set of natural numbers. X^T, X^{-1} and $\lambda_{\min}(X)$ are used to represent the transposition, inverse and minimum eigenvalue of a matrix X, respectively. $Y = \mathrm{diag}\{\cdots\}$ describes a diagonal-block matrix. The asterisk "$*$" stands for the symmetric parts in a symmetric matrix. $\delta(x)$ is a function that equals to 1 when $x = 0$ and equals to 0 otherwise. For two integers a and b, $\mathrm{mod}(a, b)$ denotes the remainder of a/b.

II. Problem Statement and Preliminaries

A. Fuzzy Systems

The following T-S fuzzy models represent a class of nonlinear systems under consideration:

Plant Rule i: **IF** $\varpi_1(s)$ is W_{i1} and $\varpi_2(s)$ is W_{i2} and $\cdots$ and $\varpi_\iota(s)$ is $W_{i\iota}$, **THEN**

$$\begin{cases} x(s+1) = A_i x(s) + B_i u(s) + E_i \omega(s) \\ \quad\; y(s) = Cx(s) + F\omega(s) \\ \quad\; z(s) = N_i x(s), \quad i \in \mathbb{T} \triangleq \{1, 2, \cdots, r\} \end{cases} \tag{1}$$

where $x(s) \in \mathbb{R}^{n_x}$ is the system state; $y(s) \triangleq [y_1(s)\ y_2(s)\ \cdots\ y_{n_y}(s)]^T \in \mathbb{R}^{n_y}$ is the measurement output; $u(s) \in \mathbb{R}^{n_u}$ is the control input; $z(s) \in \mathbb{R}^{n_z}$ is the signal to be controlled; $\omega(s) \in \mathbb{R}^{n_\omega}$ with $\omega^T(s)\omega(s) \leq \bar{\omega}^2$ is the UBB noise where $\bar{\omega}$ is a known positive scalar; $\varpi(s) \triangleq [\varpi_1(s)\ \varpi_2(s)\ \cdots\ \varpi_\iota(s)]^T$ is the measurable premise variable; W_{i1}, W_{i2}, $\cdots$, $W_{i\iota}$ are the fuzzy sets; A_i, B_i, E_i, N_i, C and F are known constant matrices; and n_x, n_y, n_u, n_z and n_ω are known positive integers.

The following compact form represents fuzzy system (1) by using the standard fuzzy inference technique:

$$\begin{cases} x(s+1) = \sum_{i=1}^{r} h_i(\varpi(s))\big(A_i x(s) + B_i u(s) + E_i \omega(s)\big) \\ \quad\; y(s) = Cx(s) + F\omega(s) \\ \quad\; z(s) = \sum_{i=1}^{r} h_i(\varpi(s)) N_i x(s) \end{cases} \tag{2}$$

where

$$h_i(\varpi(s)) \triangleq \frac{a_i(\varpi(s))}{\sum_{j=1}^{r} a_j(\varpi(s))}, \ a_i(\varpi(s)) \triangleq \prod_{j=1}^{\iota} W_{ij}(\varpi_j(s)),$$

and $W_{ij}(\varpi_j(s))$ represents the grade of membership of $\varpi_j(s)$ in fuzzy set W_{ij} $(i, j \in \mathbb{T})$. For $\forall k \in \mathbb{N}$, we have that

$$h_i(\varpi(s)) \geq 0, \quad i \in \mathbb{T}, \quad \sum_{i=1}^{r} h_i(\varpi(s)) = 1.$$

B. Communication Network

It is assumed that the information transmissions from sensors to the remote PID controller are achieved via a constrained-communication network of limited capacity. To avoid the underlying data congestion in the transmission process, the FRP is employed to determine how the network resources are used. Next, we will introduce the detailed mechanism of the FlexRay protocol and model the measurement outputs after they are transmitted through the network.

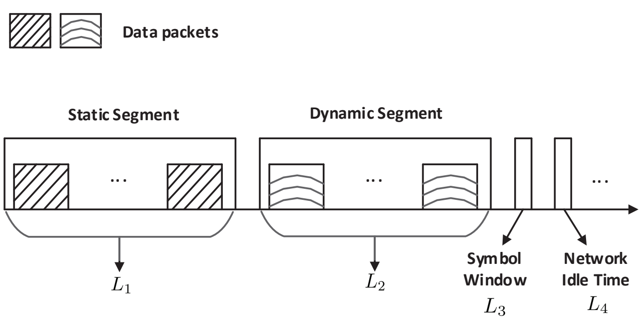

Fig. 1: Communication cycle of the FlexRay protocol

Under the scheduling of the FRP, the network communication is divided into many preset communication cycles in terms of the sampling instant. As shown in Fig. 1, each communication cycle is composed of four specific parts [35]: 1) a static segment; 2) a dynamic segment; 3) a symbol window; and 4) a network idle time. In the paper, we denote the time length of these four parts as L_1, L_2, L_3 and L_4, respectively. It is worth mentioning that, compared with the static and dynamic segments, the time lengths of the latter two parts are very short and are therefore negligible, i.e., $L_3 = L_4 = 0$ [33], [35], [36]. In addition, without loss of generality, it is assumed that $L_1 = l \leq n_y - 2$ $(l \in \mathbb{N})$ and $L_2 = \kappa$ with $l + \kappa \leq n_y$ $(\kappa \in \mathbb{N})$. Thus, the total time length of one communication cycle is $L_1 + L_2 + L_3 + L_4 = l + \kappa$.

In this paper, the time intervals of static segments are prescribed as follows:

$$\mathbb{S} \triangleq \{s | \bmod(s, l+\kappa) < l, \ s \in \mathbb{N}\}.$$

Correspondingly, the time intervals of dynamic segments are denoted by $\mathbb{D} \triangleq \mathbb{N} \setminus \mathbb{S}$.

Obviously, the static and dynamic segments play an important role in determining the network behavior with the FRP. Next, we will give a detailed description of the dynamics of the static and dynamic segments. For this purpose, some auxiliary vectors related to the measurement outputs are defined as follows:

$$y(s) \triangleq \begin{bmatrix} y^{(1)}(s) \\ y^{(2)}(s) \end{bmatrix}, \quad \bar{y}(s) \triangleq \begin{bmatrix} \bar{y}^{(1)}(s) \\ \bar{y}^{(2)}(s) \end{bmatrix},$$

$$y^{(1)}(s) \triangleq \begin{bmatrix} y_1(s) \\ y_2(s) \\ \vdots \\ y_l(s) \end{bmatrix}, \quad y^{(2)}(s) \triangleq \begin{bmatrix} y_{l+1}(s) \\ y_{l+2}(s) \\ \vdots \\ y_{n_y}(s) \end{bmatrix},$$

$$\bar{y}^{(1)}(s) \triangleq \begin{bmatrix} \bar{y}_1(s) \\ \bar{y}_2(s) \\ \vdots \\ \bar{y}_l(s) \end{bmatrix}, \quad \bar{y}^{(2)}(s) \triangleq \begin{bmatrix} \bar{y}_{l+1}(s) \\ \bar{y}_{l+2}(s) \\ \vdots \\ \bar{y}_{n_y}(s) \end{bmatrix}$$

where $\bar{y}(s)$ denotes the measurement output after they are transmitted via the network. Here, the dimension of the partial measurement output $y^{(1)}(s)$ is equal to the length of the static segment in each communication cycle. The dimension of the remaining parts of outputs (i.e., $y^{(2)}(s)$) is $n_y - l$.

In this paper, we consider the setting that the static rule (RRP) and dynamic rule (TODP) are applied, respectively, to the static segment and dynamic segment. As shown in Fig. 1, for the first L_1 time lengths in one communication cycle (corresponding to the static segment, i.e., $s \in \mathbb{S}$), the static rule is activated. Then, when it runs into the last L_2 time lengths (corresponding to the dynamic segment, i.e., $s \in \mathbb{D}$), the static rule will be shut down and the dynamic rule will be carried out immediately.

Under the protocol scheduling, only one sensor node can be chosen to access the network for data transmissions at each sampling instant. Without loss of generality, we assume that the first l components of $y(s)$ (i.e., $y^{(1)}(s)$) are orchestrated by the static rule, and the remaining components of $y(s)$ (i.e., $y^{(2)}(s)$) are scheduled by the dynamic rule. Correspondingly, $\bar{y}^{(1)}(s)$ and $\bar{y}^{(2)}(s)$ are used to denote the signal after they are transmitted. Furthermore, we denote $\sigma(s)$ (or $\tau(s)$) as the selected node at time instant k according to the static rule (or dynamic rule) which are characterized by the following mechanisms.

1) The static rule gives the same opportunities to each concerned sensor node for accessing the network, under which $\sigma(s)$ can be calculated by

$$\sigma(s) = \begin{cases} \bmod(s, l) + 1, & s \in \mathbb{S} \\ 0, & s \in \mathbb{D} \end{cases} \tag{3}$$

where $\sigma(s) \in \mathbb{L}_1 \triangleq \{1, \cdots, l\}$. It implies from (3) that, at time instant k, only the component $y_{\sigma(s)}(s)$ of $y(s)$ is updated. By means of the zero-order-holders (ZOHs) strategy, $\bar{y}_\epsilon(s)$ $(\epsilon \in \mathbb{L}_1)$ can be represented by

$$\bar{y}_\epsilon(s) = \begin{cases} y_\epsilon(s), & \epsilon = \sigma(s), \quad s \in \mathbb{S} \\ \bar{y}_\epsilon(s-1), & \epsilon \neq \sigma(s), \quad s \in \mathbb{S} \\ 0, & s \in \mathbb{D}. \end{cases} \tag{4}$$

2) The dynamic rule is an event-based dynamic scheduling algorithm, which selects sensor nodes according to node mea-

This article has been accepted for publication in a future issue of this journal, but has not been fully edited. Content may change prior to final publication. Citation information: DOI10.1109/TFUZZ.2023.3282044, IEEE Transactions on Fuzzy Systems

surement outputs during two adjacent transmission instants. Under the dynamic rule, $\tau(s)$ is determined by

$$\tau(s) = \begin{cases} \arg\max_{n=l+1,\cdots,n_y} \tilde{y}_n^T(s)Q_n\tilde{y}_n(s), & s \in \mathbb{D} \\ 0, & s \in \mathbb{S} \end{cases} \tag{5}$$

where $\tilde{y}_n(s) \triangleq y_n(s) - \bar{y}_n(s-1)$, $\tau(s) \in \mathbb{L}_2 \triangleq \{l+1, l+2, \cdots, n_y\}$ and Q_n are given positive-definite matrices. In terms of the ZOHs, $\bar{y}_n(s)$ $(n \in \mathbb{L}_2)$ can be represented by

$$\bar{y}_n(s) = \begin{cases} y_n(s), & n = \tau(s), \quad s \in \mathbb{D} \\ \bar{y}_n(s-1), & n \neq \tau(s), \quad s \in \mathbb{D} \\ 0, & s \in \mathbb{S}. \end{cases} \tag{6}$$

Without loss of generality, it is assumed that the system evolution starts from the static segment with the initial network information $\sigma(0) = 1$.

Remark 1: Under the protocol scheduling, only one node is allowed to transmit its real measurement and the latest information of other nodes is held via the ZOH strategy. By considering the switching features of the FRP, the ZOH strategy used in this paper is segment-dependent. That is to say, the ZOH in static segment is only activated when $s \in \mathbb{S}$ and shut down when $s \in \mathbb{D}$, which results in $\bar{y}_\epsilon(s) = 0$ for $\epsilon \in \mathbb{L}_1$ when $s \in \mathbb{D}$. The same is true for the dynamic segment. Such a scheme would better achieve the trade-off between data transmission quality and resource consumption.

For the further analysis, we define two auxiliary matrices:

$$\begin{aligned} \Phi_{\sigma(s)} &\triangleq \mathrm{diag}\{\delta(1-\sigma(s)), \delta(2-\sigma(s)), \cdots, \delta(l-\sigma(s))\}, \\ \Omega_{\tau(s)} &\triangleq \mathrm{diag}\{\delta(l+1-\tau(s)), \delta(l+2-\tau(s)), \\ &\qquad \cdots, \delta(n_y-\tau(s))\}. \end{aligned}$$

Based on (4) and (6), $\bar{y}^{(1)}(s)$ and $\bar{y}^{(2)}(s)$ are represented as follows:

$$\begin{aligned} \bar{y}^{(1)}(s) &= \begin{cases} \Phi_{\sigma(s)}y^{(1)}(s) + (I - \Phi_{\sigma(s)})\bar{y}^{(1)}(s-1), & s \in \mathbb{S} \\ 0, & s \in \mathbb{D} \end{cases} \\ \bar{y}^{(2)}(s) &= \begin{cases} 0, & s \in \mathbb{S} \\ \Omega_{\tau(s)}y^{(2)}(s) + (I - \Omega_{\tau(s)})\bar{y}^{(2)}(s-1), & s \in \mathbb{D}. \end{cases} \end{aligned} \tag{7}$$

Note that, there is a switching between the static segment and dynamic segment in each transmission period. By introducing a switching signal $\rho(s)$:

$$\rho(s) \triangleq \begin{cases} 0, & s \in \mathbb{S} \\ 1, & s \in \mathbb{D} \end{cases}$$

and considering (7), the compact description of $\bar{y}(s)$ is given as follows:

$$\begin{aligned} \bar{y}(s) &= \big(1-\rho(s)\big)\big(\bar{I}_1\Phi_{\sigma(s)}y^{(1)}(s) + \bar{I}_1(I - \Phi_{\sigma(s)}) \\ &\quad \times \bar{y}^{(1)}(s-1)\big) + \rho(s)\bar{I}_2\Omega_{\tau(s)}y^{(2)}(s) \\ &\quad + \rho(s)\bar{I}_2(I - \Omega_{\tau(s)})\bar{y}^{(2)}(s-1) \\ &= \Big(\big(1-\rho(s)\big)\bar{I}_1\Phi_{\sigma(s)}\bar{I}_1^T + \rho(s)\bar{I}_2\Omega_{\tau(s)}\bar{I}_2^T\Big)y(s) \\ &\quad + \Big(\big(1-\rho(s)\big)\bar{I}_1(I - \Phi_{\sigma(s)})\bar{I}_1^T \\ &\quad + \rho(s)\bar{I}_2(I - \Omega_{\tau(s)})\bar{I}_2^T\Big)\bar{y}(s-1) \end{aligned} \tag{8}$$

where

$$\bar{I}_1 \triangleq \begin{bmatrix} I_l \\ 0_{(n_y-l)\times l} \end{bmatrix}, \quad \bar{I}_2 \triangleq \begin{bmatrix} 0_{l\times(n_y-l)} \\ I_{(n_y-l)} \end{bmatrix}.$$

C. PID Controller

Based on the available measurement $\bar{y}(s)$, the following fuzzy PID controller is adopted:

$$\begin{aligned} u(s) = \sum_{j=1}^{r} h_j(\bar{\varpi}(s))\Big(&K_j^P\bar{y}(s) + K_j^I\sum_{\pi=s-N}^{s-1}\bar{y}(\pi) \\ &+ K_j^D(\bar{y}(s) - \bar{y}(s-1))\Big) \end{aligned} \tag{9}$$

where $\bar{\varpi}(s)$ is the premise variable of the controller; K_j^P, K_j^I and K_j^D are controller gains; and N $(N \geq 2)$ is a given positive integer which represents the length of the integral (accumulative) time window.

Remark 2: The features of the proposed fuzzy PID controller are highlighted as twofold: 1) in the integral (accumulative) term, a time window is introduced to use the past information with finite time length, which is helpful in improving the calculation efficiency; and 2) due to the utilization of the FRP, the premise variable $\varpi(s)$ may not be available in real-time, and thus, a different premise variable $\bar{\varpi}(s)$ is used to facilitate the implementation of the fuzzy controller.

Now, we define two auxiliary vectors:

$$\begin{aligned} \eta(s) &\triangleq \begin{bmatrix} x^T(s) & \bar{y}^T(s-1) \end{bmatrix}^T, \\ \bar{\eta}(s) &\triangleq \begin{bmatrix} \eta^T(s-1) & \eta^T(s-2) & \cdots & \eta^T(s-N+1) \end{bmatrix}^T. \end{aligned}$$

In order to save space, we further denote

$$\sigma \triangleq \sigma(s), \ \tau \triangleq \tau(s).$$

Then, by considering (2), (8) and (9) simultaneously, the closed-loop system is obtained as follows:

$$\begin{cases} \eta(s+1) = \sum_{i=1}^{r}\sum_{j=1}^{r} h_i(\varpi(s))h_j(\bar{\varpi}(s))\Big(\mathcal{A}_{i,j,\sigma,\tau}(s)\eta(s) \\ \qquad\qquad + \mathcal{B}_{i,j}\bar{\eta}(s) + \mathcal{E}_{i,j,\sigma,\tau}(s)\omega(s)\Big) \\ \quad z(s) = \sum_{i=1}^{r} h_i(\varpi(s))\mathcal{N}_i\eta(s) \end{cases} \tag{10}$$

where

$$\begin{aligned} \mathcal{A}_{i,j,\sigma,\tau}(s) &\triangleq \begin{bmatrix} \mathcal{A}_{i,j,\sigma,\tau}^{(1,1)}(s) & \mathcal{A}_{i,j,\sigma,\tau}^{(1,2)}(s) \\ \hat{\Phi}_{\sigma,\tau}(s)C & \bar{\Phi}_{\sigma,\tau}(s) \end{bmatrix}, \\ \mathcal{A}_{i,j,\sigma,\tau}^{(1,1)}(s) &\triangleq A_i + B_iK_j^P\hat{\Phi}_{\sigma,\tau}(s)C + B_iK_j^D\hat{\Phi}_{\sigma,\tau}(s)C, \\ \mathcal{A}_{i,j,\sigma,\tau}^{(1,2)}(s) &\triangleq B_iK_j^P\bar{\Phi}_{\sigma,\tau}(s) + B_iK_j^D\bar{\Phi}_{\sigma,\tau}(s) \\ &\quad + B_iK_j^I - B_iK_j^D, \\ \hat{\Phi}_{\sigma,\tau}(s) &\triangleq \big(1-\rho(s)\big)\bar{I}_1\Phi_\sigma\bar{I}_1^T + \rho(s)\bar{I}_2\Omega_\tau\bar{I}_2^T, \\ \bar{\Phi}_{\sigma,\tau}(s) &\triangleq \big(1-\rho(s)\big)\bar{I}_1(I-\Phi_\sigma)\bar{I}_1^T \\ &\quad + \rho(s)\bar{I}_2(I-\Omega_\tau)\bar{I}_2^T, \\ \mathcal{B}_{i,j} &\triangleq \big[\underbrace{\tilde{B}_{i,j} \ \ \tilde{B}_{i,j} \ \ \cdots \ \ \tilde{B}_{i,j}}_{N-1}\big], \quad \mathcal{N}_i \triangleq \begin{bmatrix} N_i & 0 \end{bmatrix}, \\ \tilde{B}_{i,j} &\triangleq \begin{bmatrix} 0 & B_iK_j^I \\ 0 & 0 \end{bmatrix}, \quad \mathcal{E}_{i,j,\sigma,\tau}(s) \triangleq \begin{bmatrix} \mathcal{E}_{i,j,\sigma,\tau}^{(1,1)}(s) \\ \hat{\Phi}_{\sigma,\tau}(s)F \end{bmatrix}, \end{aligned}$$

This article has been accepted for publication in a future issue of this journal, but has not been fully edited. Content may change prior to final publication. Citation information: DOI10.1109/TFUZZ.2023.3282044, IEEE Transactions on Fuzzy Systems

$$\mathcal{E}^{(1,1)}_{i,j\sigma,\tau}(s) \triangleq E_i + B_iK_j^P\hat{\Phi}_{\sigma,\tau}(s)F + B_iK_j^D\hat{\Phi}_{\sigma,\tau}(s)F.$$

Definition 1: [55] Exponentially ultimate boundedness of the closed-loop system (10) is defined as the existence of constants $a \in [0,1)$, $b > 0$, and $c > 0$ satisfying

$$\|\eta(s)\|^2 \leq a^s b + c$$

where a and c denote the decay rate and the asymptotic upper bound (AUB) of $\eta(s)$, respectively.

This paper aims to design a fuzzy PID controller for fuzzy system (2) that satisfies the following requirements simultaneously.

R1) Ensure the ultimate boundedness of the closed-loop system (10) subject to the noise $\omega(s)$.

R2) Minimize the AUB of the controlled output $\|z(s)\|$ by the designed controller gain matrices K_j^P, K_j^I, and K_j^D.

III. Main Results

The main focus of this section is on the performance analysis for system (10) and the design of the fuzzy PID controller under the effects of the FRP and UBB noises.

To obtain the protocol-affected boundedness results, let's define a new time-sequence according to the features of the FRP:

$$t(\varepsilon) \triangleq \varepsilon(l+\kappa) + l, \quad \varepsilon = 0, 1, 2, \cdots$$

where l and κ are, respectively, the time lengths of the static and the dynamic segments in each communication cycle. That is, $t(\varepsilon)$ is the first time-instant in the dynamic segment in the $(\varepsilon+1)$th communication cycle. An example with $L_1 = l = 3$ and $L_2 = \kappa = 2$ is given in Fig. 2 where $t(0) = 3$, $t(1) = 8$, $\cdots$.

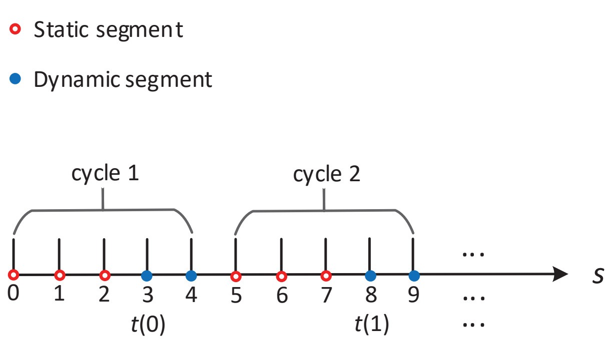

Fig. 2: Time sequence of $t(\varepsilon)$

The introduction of $t(\varepsilon)$ enables us to check the system property in each communication cycle, and further discuss the boundedness over the entire time domain.

The following theorem establishes sufficient conditions to guarantee the boundedness of the system variables $\eta(s)$ and $z(s)$ based on the switching-system theory and the newly introduced time-sequence $t(\varepsilon)$.

Theorem 1: Consider the closed-loop fuzzy system (10) with the PID controller (9). Let the controller gains and scalars $\mu_1 > -1$, $\mu_2 > -1$ be given. Then, the dynamics of the closed-loop system (10) is ultimately bounded if, for $i, j \in \mathbb{T}$, $d = 1, 2, \cdots, N-1$, $\epsilon \in \mathbb{L}_1$, $n \in \mathbb{L}_2$, there are positive matrices $P > 0$, $R_d > 0$ and scalars $o_{1,n} > 0$, $o_{2,n} > 0$, $\alpha_1 > 0$, $\alpha_2 > 0$ such that

$$\Lambda_n + \Theta^T_{i,j,n}\bar{P}\Theta_{i,j,n} < 0 \tag{11}$$
$$\Lambda_n + \Theta^T_{i,j,n}P\Theta_{i,j,n} < 0 \tag{12}$$
$$\Xi + \Gamma^T_{i,j,\epsilon}P\Gamma_{i,j,\epsilon} < 0 \tag{13}$$
$$\Xi + \Gamma^T_{i,j,\epsilon}\tilde{P}\Gamma_{i,j,\epsilon} < 0 \tag{14}$$
$$(1+\mu_1)^\kappa(1+\mu_2)^l < 1 \tag{15}$$
$$\sum_{\bar{n}=l+1}^{n_y} o_{1,\bar{n}} = 1 \tag{16}$$
$$\sum_{\bar{n}=l+1}^{n_y} o_{2,\bar{n}} = 1 \tag{17}$$

where

$$\begin{aligned}
\Lambda_n &\triangleq \mathrm{diag}\{\Lambda_n^{(1)}, -\bar{R}, -\alpha_2 I\},\\
\Lambda_n^{(1)} &\triangleq -(1+\mu_1)P - (1+\mu_1)\tilde{C}^T\vec{Q}_n\tilde{C} + \tilde{R},\\
\tilde{R} &\triangleq \begin{bmatrix} \sum_{d=1}^{N-1} R_d & 0 \\ 0 & -\alpha_1 I \end{bmatrix}, \quad \Xi^{(1)} \triangleq -(1+\mu_2)P + \tilde{R},\\
\bar{R} &\triangleq \mathrm{diag}\{\bar{\mu}R_1, \bar{\mu}^2R_2, \cdots, \bar{\mu}^{N-1}R_{N-1}\},\\
\tilde{C} &\triangleq \bar{I}_2^T \begin{bmatrix} C & -I & F \end{bmatrix}, \quad \bar{\mu} \triangleq \min\{1+\mu_1, 1+\mu_2\},\\
\vec{Q}_n &\triangleq \bar{Q} - \bar{Q}\Omega_n, \quad \bar{Q} \triangleq \mathrm{diag}\{Q_{l+1}, Q_{l+2}, \cdots, Q_{n_y}\},\\
\Theta_{i,j,n} &\triangleq \begin{bmatrix} \bar{A}_{i,j,n} & \bar{E}_{i,j,n} & \mathcal{B}_{i,j} & 0 \\ 0 & 0 & 0 & I \end{bmatrix},\\
\bar{A}_{i,j,n} &\triangleq \begin{bmatrix} \bar{A}^{(1,1)}_{i,j,n} & \bar{A}^{(1,2)}_{i,j,n} \\ \bar{I}_2\Omega_n\bar{I}_2^TC & \tilde{\Phi}_n \end{bmatrix}, \quad \tilde{\Phi}_n \triangleq \bar{I}_2(I-\Omega_n)\bar{I}_2^T,\\
\bar{A}^{(1,1)}_{i,j,n} &\triangleq A_i + B_iK_j^P\bar{I}_2\Omega_n\bar{I}_2^TC + B_iK_j^D\bar{I}_2\Omega_n\bar{I}_2^TC,\\
\bar{A}^{(1,2)}_{i,j,n} &\triangleq B_iK_j^P\tilde{\Phi}_n + B_iK_j^D\tilde{\Phi}_n + B_iK_j^I - B_iK_j^D,\\
\bar{P} &\triangleq P + \sum_{\bar{n}=l+1}^{n_y} o_{1,\bar{n}}\tilde{C}^T\vec{Q}_{\bar{n}}\tilde{C},\\
\Xi &\triangleq \mathrm{diag}\{\Xi^{(1)}, -\bar{R}, -\alpha_2 I\},\\
\Gamma_{i,j,\epsilon} &\triangleq \begin{bmatrix} \check{A}_{i,j,\epsilon} & \check{E}_{i,j,\epsilon} & \mathcal{B}_{i,j} & 0 \\ 0 & 0 & 0 & I \end{bmatrix},\\
\check{A}_{i,j,\epsilon} &\triangleq \begin{bmatrix} \check{A}^{(1,1)}_{i,j,\epsilon} & \check{A}^{(1,2)}_{i,j,\epsilon} \\ \bar{I}_1\Phi_\epsilon\bar{I}_1^TC & \vec{\Phi}_\epsilon \end{bmatrix}, \quad \vec{\Phi}_\epsilon \triangleq \bar{I}_1(I-\Phi_\epsilon)\bar{I}_1^T,\\
\check{A}^{(1,1)}_{i,j,\epsilon} &\triangleq A_i + B_iK_j^P\bar{I}_1\Phi_\epsilon\bar{I}_1^TC + B_iK_j^D\bar{I}_1\Phi_\epsilon\bar{I}_1^TC,\\
\check{A}^{(1,2)}_{i,j,n} &\triangleq B_iK_j^P\vec{\Phi}_\epsilon + B_iK_j^D\vec{\Phi}_\epsilon + B_iK_j^I - B_iK_j^D,\\
\tilde{P} &\triangleq P + \sum_{\bar{n}=l+1}^{n_y} o_{2,\bar{n}}\tilde{C}^T\vec{Q}_{\bar{n}}\tilde{C},\\
\bar{E}_{i,j,n} &\triangleq \begin{bmatrix} \bar{E}^{(1,1)}_{i,j,n} \\ \bar{I}_2\Omega_n\bar{I}_2^TF \end{bmatrix}, \quad \check{E}_{i,j,n} \triangleq \begin{bmatrix} \check{E}^{(1,1)}_{i,j,\epsilon} \\ \bar{I}_1\Phi_\epsilon\bar{I}_1^TF \end{bmatrix},\\
\bar{E}^{(1,1)}_{i,j,\epsilon} &\triangleq E_i + B_iK_j^P\bar{I}_2\Omega_n\bar{I}_2^TF + B_iK_j^D\bar{I}_2\Omega_n\bar{I}_2^TF,\\
\check{E}^{(1,1)}_{i,j,\epsilon} &\triangleq E_i + B_iK_j^P\bar{I}_1\Phi_\epsilon\bar{I}_1^TF + B_iK_j^D\bar{I}_1\Phi_\epsilon\bar{I}_1^TF.
\end{aligned}$$

Proof: Choose the following Lyapunov-like functional:

$$V(s) \triangleq V_1(s) + V_2(s)$$

where

$$V_1(s) \triangleq \begin{bmatrix}\eta(s)\\ \omega(s)\end{bmatrix}^T \left(P + \rho(s)\tilde{C}^T\vec{Q}_{\tau(s)}\tilde{C}\right)\begin{bmatrix}\eta(s)\\ \omega(s)\end{bmatrix},$$
$$V_2(s) \triangleq \sum_{d=1}^{N-1}\sum_{p=s-d}^{s-1}\bar{\mu}^{s-p-1}\eta^T(p)R_d\eta(p).$$

For $\bar{n} \in \mathbb{L}_2$, one can derive from the definition of $\vec{Q}_n$ and the selection principle (5) that:

$$\begin{bmatrix}\eta(s+1)\\ \omega(s+1)\end{bmatrix}^T \tilde{C}^T\vec{Q}_{\tau(s+1)}\tilde{C}\begin{bmatrix}\eta(s+1)\\ \omega(s+1)\end{bmatrix} \leq \begin{bmatrix}\eta(s+1)\\ \omega(s+1)\end{bmatrix}^T \tilde{C}^T\vec{Q}_{\bar{n}}\tilde{C}\begin{bmatrix}\eta(s+1)\\ \omega(s+1)\end{bmatrix}. \tag{18}$$

Next, we will discuss four different cases according to the time-sequence $t(\varepsilon)$.

Case 1: For $s \in \{t(\varepsilon), t(\varepsilon)+1, \cdots, t(\varepsilon)+\kappa-2\} \in \mathbb{D}$, one has that $s+1 \in \{t(\varepsilon)+1, t(\varepsilon)+2, \cdots, t(\varepsilon)+\kappa-1\} \in \mathbb{D}$ and

$$\begin{aligned}
&V_1(s+1) - (1+\mu_1)V_1(s)\\
&= \begin{bmatrix}\eta(s+1)\\ \omega(s+1)\end{bmatrix}^T \left(P + \rho(s+1)\tilde{C}^T\vec{Q}_{\tau(s+1)}\tilde{C}\right)\begin{bmatrix}\eta(s+1)\\ \omega(s+1)\end{bmatrix}\\
&\quad - (1+\mu_1)\begin{bmatrix}\eta(s)\\ \omega(s)\end{bmatrix}^T \left(P + \rho(s)\tilde{C}^T\vec{Q}_{\tau(s)}\tilde{C}\right)\begin{bmatrix}\eta(s)\\ \omega(s)\end{bmatrix}\\
&\leq \begin{bmatrix}\eta(s+1)\\ \omega(s+1)\end{bmatrix}^T \left(P + \sum_{\bar{n}=l+1}^{n_y} o_{1,\bar{n}}\tilde{C}^T\vec{Q}_{\bar{n}}\tilde{C}\right)\begin{bmatrix}\eta(s+1)\\ \omega(s+1)\end{bmatrix}\\
&\quad - (1+\mu_1)\begin{bmatrix}\eta(s)\\ \omega(s)\end{bmatrix}^T \left(P + \rho(s)\tilde{C}^T\vec{Q}_{\tau(s)}\tilde{C}\right)\begin{bmatrix}\eta(s)\\ \omega(s)\end{bmatrix}.
\end{aligned} \tag{19}$$

By considering (18) and the fact of

$$\alpha_1\omega^T(s)\omega(s) \leq \alpha_1\bar{\omega}^2,$$
$$\alpha_2\omega^T(s+1)\omega(s+1) \leq \alpha_2\bar{\omega}^2,$$

one obtains

$$\begin{aligned}
&V_1(s+1) - (1+\mu_1)V_1(s)\\
&\leq \begin{bmatrix}\eta(s+1)\\ \omega(s+1)\end{bmatrix}^T \left(P + \sum_{\bar{n}=l+1}^{n_y} o_{1,\bar{n}}\tilde{C}^T\vec{Q}_{\bar{n}}\tilde{C}\right)\begin{bmatrix}\eta(s+1)\\ \omega(s+1)\end{bmatrix}\\
&\quad - (1+\mu_1)\begin{bmatrix}\eta(s)\\ \omega(s)\end{bmatrix}^T \left(P + \rho(s)\tilde{C}^T\vec{Q}_{\tau(s)}\tilde{C}\right)\begin{bmatrix}\eta(s)\\ \omega(s)\end{bmatrix}\\
&\quad + (\alpha_1+\alpha_2)\bar{\omega}^2 - \alpha_1\omega^T(s)\omega(s)\\
&\quad - \alpha_2\omega^T(s+1)\omega(s+1).
\end{aligned} \tag{20}$$

Letting $\tau(s) = n$ ($n \in \mathbb{L}_2$), one has

$$\begin{aligned}
&V_1(s+1) - (1+\mu_1)V_1(s)\\
&\leq \sum_{i=1}^{r}\sum_{j=1}^{r} h_i(\varpi(s))h_j(\bar{\varpi}(s))\xi^T(s)\left(\Theta_{i,j,n}^T\bar{P}\Theta_{i,j,n} + \bar{\Lambda}_n\right)\\
&\quad \times \xi(s) + (\alpha_1+\alpha_2)\bar{\omega}^2
\end{aligned} \tag{21}$$

where

$$\bar{\alpha}_1 \triangleq \begin{bmatrix}0 & 0\\ 0 & -\alpha_1 I\end{bmatrix},$$
$$\xi(s) \triangleq \begin{bmatrix}\eta(s) & \omega(s) & \bar{\eta}(s) & \omega(s+1)\end{bmatrix}^T,$$
$$\bar{\Lambda}_n \triangleq \begin{bmatrix}-(1+\mu_1)(P+\tilde{C}^T\vec{Q}_n\tilde{C}) + \bar{\alpha}_1 & 0 & 0\\ 0 & 0 & 0\\ 0 & 0 & -\alpha_2 I\end{bmatrix}.$$

For $V_2(s)$, we calculate that

$$\begin{aligned}
&V_2(s+1) - (1+\mu_1)V_2(s)\\
&\leq V_2(s+1) - \bar{\mu}V_2(s)\\
&= \sum_{d=1}^{N-1}\sum_{p=s-d+1}^{s}\bar{\mu}^{s-p}\eta^T(p)R_d\eta(p)\\
&\quad - \sum_{d=1}^{N-1}\sum_{p=s-d}^{s-1}\bar{\mu}^{s-p}\eta^T(p)R_d\eta(p)\\
&= \sum_{d=1}^{N-1}\eta^T(s)R_d\eta(s) - \sum_{d=1}^{N-1}\bar{\mu}^d\eta^T(s-d)R_d\eta(s-d).
\end{aligned} \tag{22}$$

Together (21) with (22), one obtains

$$\begin{aligned}
&V(s+1) - (1+\mu_1)V(s)\\
&\leq \sum_{i=1}^{r}\sum_{j=1}^{r} h_i(\varpi(s))h_j(\bar{\varpi}(s))\xi^T(s)\left(\Theta_{i,j,n}^T\bar{P}\Theta_{i,j,n} + \Lambda_n\right)\\
&\quad \times \xi(s) + (\alpha_1+\alpha_2)\bar{\omega}^2.
\end{aligned} \tag{23}$$

The condition (11) implies

$$V(s+1) - (1+\mu_1)V(s) \leq (\alpha_1+\alpha_2)\bar{\omega}^2. \tag{24}$$

Case 2: For $s = t(\varepsilon)+\kappa-1 \in \mathbb{D}$, one has that $s+1 = t(\varepsilon)+\kappa \in \mathbb{S}$ and

$$\begin{aligned}
&V(s+1) - (1+\mu_1)V(s)\\
&= \begin{bmatrix}\eta(s+1)\\ \omega(s+1)\end{bmatrix}^T P\begin{bmatrix}\eta(s+1)\\ \omega(s+1)\end{bmatrix} - (1+\mu_1)\begin{bmatrix}\eta(s)\\ \omega(s)\end{bmatrix}^T\\
&\quad \times \left(P + \rho(s)\tilde{C}^T\vec{Q}_{\tau(s)}\tilde{C}\right)\begin{bmatrix}\eta(s)\\ \omega(s)\end{bmatrix} + V_2(s+1)\\
&\quad - (1+\mu_1)V_2(s).
\end{aligned} \tag{25}$$

By following the similar analysis method and using the condition (12), we arrive at

$$V(s+1) - (1+\mu_1)V(s) \leq (\alpha_1+\alpha_2)\bar{\omega}^2. \tag{26}$$

Thus, for $s \in \mathbb{D}$ and any scalar $\upsilon > 0$, one has that

$$\begin{aligned}
&\upsilon^{s+1}V(s+1) - \upsilon^s V(s)\\
&= \upsilon^{s+1}\big(V(s+1) - V(s)\big) + \upsilon^s(\upsilon-1)V(s)\\
&\leq \upsilon^{s+1}\big(\mu_1 V(s) + (\alpha_1+\alpha_2)\bar{\omega}^2\big) + \upsilon^s(\upsilon-1)V(s)\\
&= \upsilon^s(\mu_1\upsilon + \upsilon - 1)V(s) + \upsilon^{s+1}(\alpha_1+\alpha_2)\bar{\omega}^2.
\end{aligned}$$

By letting $\bar{\upsilon} \triangleq \frac{1}{1+\mu_1}$, one derives

$$\bar{\upsilon}^{s+1}V(s+1) - \bar{\upsilon}^s V(s) \leq \bar{\upsilon}^{s+1}(\alpha_1+\alpha_2)\bar{\omega}^2.$$

Summing up both sides of the above inequality from $s = t(\varepsilon)$ to $s = t(\varepsilon)+\kappa-1$, one infers

$$\begin{aligned}
&\bar{\upsilon}^{t(\varepsilon)+\kappa}V(t(\varepsilon)+\kappa) - \bar{\upsilon}^{t(\varepsilon)}V(t(\varepsilon))\\
&\leq \frac{\bar{\upsilon}^{t(\varepsilon)+1} - \bar{\upsilon}^{t(\varepsilon)+1+\kappa}}{1-\bar{\upsilon}}(\alpha_1+\alpha_2)\bar{\omega}^2.
\end{aligned}$$

This article has been accepted for publication in a future issue of this journal, but has not been fully edited. Content may change prior to final publication. Citation information: DOI10.1109/TFUZZ.2023.3282044, IEEE Transactions on Fuzzy Systems

Thus, it can be concluded that

$$V(t(\varepsilon)+\kappa) \leq \bar{\upsilon}^{-\kappa} V(t(\varepsilon)) + \frac{\bar{\upsilon}^{1-\kappa}-\bar{\upsilon}}{1-\bar{\upsilon}}(\alpha_1+\alpha_2)\bar{\omega}^2. \quad (27)$$

Case 3: For $s \in \{t(\varepsilon)+\kappa, t(\varepsilon)+\kappa+1, \cdots, t(\varepsilon+1)-2\} \in \mathbb{S}$, one has that $s+1 \in \{t(\varepsilon)+\kappa+1, t(\varepsilon)+\kappa+2, \cdots, t(\varepsilon+1)-1\} \in \mathbb{S}$ and

$$\begin{aligned} &V_1(s+1)-(1+\mu_2)V_1(s) \\ &= \begin{bmatrix}\eta(s+1)\\ \omega(s+1)\end{bmatrix}^T P \begin{bmatrix}\eta(s+1)\\ \omega(s+1)\end{bmatrix} \\ &\quad -(1+\mu_2)\begin{bmatrix}\eta(s)\\ \omega(s)\end{bmatrix}^T P \begin{bmatrix}\eta(s)\\ \omega(s)\end{bmatrix}, \end{aligned}$$

and

$$\begin{aligned} &V_2(s+1)-(1+\mu_2)V_2(s) \\ &\leq V_2(s+1)-\bar{\mu}V_2(s) \\ &= \sum_{d=1}^{N-1}\sum_{p=s-d+1}^{s} \bar{\mu}^{s-p}\eta^T(p)R_d\eta(p) \\ &\quad - \sum_{d=1}^{N-1}\sum_{p=s-d}^{s-1} \bar{\mu}^{s-p}\eta^T(p)R_d\eta(p) \\ &= \sum_{d=1}^{N-1}\eta^T(s)R_d\eta(s) - \sum_{d=1}^{N-1}\bar{\mu}^d\eta^T(s-d)R_d\eta(s-d). \end{aligned}$$

Thus, we have

$$\begin{aligned} &V(s+1)-(1+\mu_2)V(s) \\ &\leq \sum_{i=1}^{r}\sum_{j=1}^{r} h_i(\varpi(s))h_j(\bar{\varpi}(s))\xi^T(s)\big(\Xi+\Gamma_{i,j,\epsilon}^T P\Gamma_{i,j,\epsilon}\big)\xi(s) \\ &\quad +(\alpha_1+\alpha_2)\bar{\omega}^2. \end{aligned}$$

Under the condition (13), it is easy to see that

$$V(s+1)-(1+\mu_2)V(s) \leq (\alpha_1+\alpha_2)\bar{\omega}^2.$$

Case 4: For $s = t(\varepsilon+1)-1 \in \mathbb{S}$, one has that $s+1 = t(\varepsilon+1) \in \mathbb{D}$ and

$$\begin{aligned} &V(s+1)-(1+\mu_2)V(s) \\ &= \begin{bmatrix}\eta(s+1)\\ \omega(s+1)\end{bmatrix}^T \left(P+\rho(s+1)\tilde{C}^T\vec{Q}_{\tau(s+1)}\tilde{C}\right)\begin{bmatrix}\eta(s+1)\\ \omega(s+1)\end{bmatrix} \\ &\quad -(1+\mu_2)\begin{bmatrix}\eta(s)\\ \omega(s)\end{bmatrix}^T P \begin{bmatrix}\eta(s)\\ \omega(s)\end{bmatrix} + V_2(s+1) \\ &\quad -(1+\mu_2)V_2(s) \\ &\leq \begin{bmatrix}\eta(s+1)\\ \omega(s+1)\end{bmatrix}^T \left(P+\sum_{\bar{n}=1}^{n_y} o_{2,\bar{n}}\tilde{C}^T\vec{Q}_{\bar{n}}\tilde{C}\right)\begin{bmatrix}\eta(s+1)\\ \omega(s+1)\end{bmatrix} \\ &\quad -(1+\mu_2)\begin{bmatrix}\eta(s)\\ \omega(s)\end{bmatrix}^T P \begin{bmatrix}\eta(s)\\ \omega(s)\end{bmatrix} + V_2(s+1)-\bar{\mu}V_2(s) \\ &\leq \sum_{i=1}^{r}\sum_{j=1}^{r} h_i(\varpi(s))h_j(\bar{\varpi}(s))\xi^T(s)\big(\Xi+\Gamma_{i,j,\epsilon}^T\tilde{P}\Gamma_{i,j,\epsilon}\big)\xi(s) \\ &\quad +(\alpha_1+\alpha_2)\bar{\omega}^2. \end{aligned}$$

Based on the condition (14), we know that the following holds:

$$V(s+1)-(1+\mu_2)V(s) \leq (\alpha_1+\alpha_2)\bar{\omega}^2.$$

Therefore, for $s \in \mathbb{S}$ and any scalar $\varsigma > 0$, one obtains that

$$\begin{aligned} &\varsigma^{s+1}V(s+1)-\varsigma^s V(s) \\ &= \varsigma^{s+1}\big(V(s+1)-V(s)\big)+\varsigma^s(\varsigma-1)V(s) \\ &\leq \varsigma^{s+1}\big(\mu_2 V(s)+(\alpha_1+\alpha_2)\bar{\omega}^2\big)+\varsigma^s(\varsigma-1)V(s) \\ &= \varsigma^s(\mu_2\varsigma+\varsigma-1)V(s)+\varsigma^{s+1}(\alpha_1+\alpha_2)\bar{\omega}^2. \end{aligned}$$

By letting $\bar{\varsigma} \triangleq \frac{1}{\mu_2+1}$, it can infer from the above formula that

$$\bar{\varsigma}^{s+1}V(s+1)-\bar{\varsigma}^s V(s) \leq \bar{\varsigma}^{s+1}(\alpha_1+\alpha_2)\bar{\omega}^2.$$

Summing up both sides of the above inequality from $s = t(\varepsilon)+\kappa$ to $s = t(\varepsilon+1)-1$ gives that

$$\begin{aligned} &\bar{\varsigma}^{t(\varepsilon+1)}V(t(\varepsilon+1)) - \bar{\varsigma}^{t(\varepsilon)+\kappa}V(t(\varepsilon)+\kappa) \\ &\leq \frac{\bar{\varsigma}^{t(\varepsilon)+\kappa+1}-\bar{\varsigma}^{t(\varepsilon)+1+\kappa+l}}{1-\bar{\varsigma}}(\alpha_1+\alpha_2)\bar{\omega}^2. \end{aligned}$$

Thus, it can be concluded that

$$V(t(\varepsilon+1)) \leq \bar{\varsigma}^{-l}V(t(\varepsilon)+\kappa) + \frac{\bar{\varsigma}^{1-l}-\bar{\varsigma}}{1-\bar{\varsigma}}(\alpha_1+\alpha_2)\bar{\omega}^2. \quad (28)$$

In terms of (27) and (28), one gets

$$V(t(\varepsilon+1)) \leq \gamma V(t(\varepsilon)) + \breve{\alpha}\bar{\omega}^2 \quad (29)$$

where

$$\begin{aligned} \gamma &\triangleq (1+\mu_1)^\kappa(1+\mu_2)^l, \\ \breve{\alpha} &\triangleq \left(\frac{\bar{\varsigma}^{-l}\bar{\upsilon}^{1-\kappa}-\bar{\varsigma}^{-l}\bar{\upsilon}}{1-\bar{\upsilon}}+\frac{\bar{\varsigma}^{1-l}-\bar{\varsigma}}{1-\bar{\varsigma}}\right)(\alpha_1+\alpha_2). \end{aligned}$$

Thus, for any scalar $\pi > 0$, one has

$$\begin{aligned} &\pi^{\varepsilon+1}V(t(\varepsilon+1)) - \pi^\varepsilon V(t(\varepsilon)) \\ &\leq \pi^\varepsilon(\pi\gamma-1)V(t(\varepsilon)) + \pi^{\varepsilon+1}\breve{\alpha}\bar{\omega}^2. \end{aligned}$$

By letting $\bar{\pi} \triangleq \frac{1}{\gamma}$ and summing up both sides of the above inequality from $\bar{\varepsilon} = 0$ to $\bar{\varepsilon} = \varepsilon-1$, one has

$$V(t(\varepsilon)) \leq \bar{\pi}^{-\varepsilon}V(t(0)) + \frac{\bar{\pi}^{1-\varepsilon}-\bar{\pi}}{1-\bar{\pi}}\breve{\alpha}\bar{\omega}^2.$$

Combining with (28), one knows

$$V(t(0)) \leq \bar{\varsigma}^{-l}V(0) + \vec{\alpha}\bar{\omega}^2 \triangleq \bar{V}(0)$$

where

$$\vec{\alpha} \triangleq \frac{\bar{\varsigma}^{1-l}-\bar{\varsigma}}{1-\bar{\varsigma}}(\alpha_1+\alpha_2).$$

Thus, one has that

$$\begin{aligned} V(t(\varepsilon)) &\leq \bar{\pi}^{-\varepsilon}\bar{V}(0) + \frac{\bar{\pi}^{1-\varepsilon}-\bar{\pi}}{1-\bar{\pi}}\breve{\alpha}\bar{\omega}^2 \\ &= \gamma^\varepsilon\left(\bar{V}(0)+\frac{\breve{\alpha}\bar{\omega}^2}{\gamma-1}\right)+\frac{\breve{\alpha}\bar{\omega}^2}{1-\gamma}. \end{aligned}$$

This article has been accepted for publication in a future issue of this journal, but has not been fully edited. Content may change prior to final publication. Citation information: DOI10.1109/TFUZZ.2023.3282044, IEEE Transactions on Fuzzy Systems

Under the condition (15), it is easy to see that $V(t(\varepsilon)) \to \frac{\breve{\alpha}\bar{\varpi}^2}{1-\gamma} < \infty$ as $\varepsilon \to \infty$, which shows the boundedness of the dynamics of $V(t(\varepsilon))$.

After discussing the dynamics of $V(t(\varepsilon))$, we are now in a position to check the properties of dynamics of $V(s)$ (for $s \in \mathbb{N}$). Note that the condition (15) implies three different cases:

1) $1+\mu_1 < 1$ and $1+\mu_2 > 1$;
2) $1+\mu_1 < 1$ and $1+\mu_2 < 1$;
3) $1+\mu_1 > 1$ and $1+\mu_2 < 1$.

According to the values of μ_1 and μ_2, we next discuss the boundedness of $V(s)$ in three cases, respectively.

Case a: If $1+\mu_1 < 1$ and $1+\mu_2 > 1$, then for $s \in \{t(\varepsilon), t(\varepsilon)+1, \cdots, t(\varepsilon)+\kappa\}$, one has from (27) that

$$V(s) \le V(t(\varepsilon)) + \frac{\bar{\upsilon}^{1-\kappa} - \bar{\upsilon}}{1-\bar{\upsilon}}(\alpha_1+\alpha_2)\bar{\varpi}^2.$$

For $s \in \{t(\varepsilon)+\kappa+1, t(\varepsilon)+\kappa+2, \cdots, t(\varepsilon+1)-1\}$, one has from (28) and (29) that

$$\begin{aligned} V(s) \le& \bar{\varsigma}^{1-l}\bar{\upsilon}^{-\kappa}V(t(\varepsilon)) + \acute{\alpha}\bar{\varpi}^2 \\ \le& \bar{\varsigma}^{-l}\bar{\upsilon}^{-\kappa}V(t(\varepsilon)) + \acute{\alpha}\bar{\varpi}^2 \\ \le& V(t(\varepsilon)) + \acute{\alpha}\bar{\varpi}^2 \end{aligned}$$

where

$$\acute{\alpha} \triangleq \left(\frac{\bar{\varsigma}^{1-l}\bar{\upsilon}^{1-\kappa} - \bar{\varsigma}^{1-l}\bar{\upsilon}}{1-\bar{\upsilon}} + \frac{\bar{\varsigma}^{2-l} - \bar{\varsigma}}{1-\bar{\varsigma}}\right)(\alpha_1+\alpha_2).$$

Therefore, for $s \in \{t(\varepsilon), t(\varepsilon)+1, \cdots, t(\varepsilon+1)-1\}$, it follows from the above inequalities that

$$V(s) \le V(t(\varepsilon)) + \acute{\alpha}\bar{\varpi}^2.$$

To this end, it is concluded as $s \to +\infty$ that

$$\begin{aligned} \|\eta(s)\|^2 \le& V_1(s)/\bar{p} \\ \le& \big(V(t(\varepsilon)) + \acute{\alpha}\bar{\varpi}^2\big)/\bar{p} \\ \le& \frac{\breve{\alpha}\bar{\varpi}^2}{(1-\gamma)\bar{p}} + \frac{\acute{\alpha}\bar{\varpi}^2}{\bar{p}} < \infty \end{aligned} \tag{30}$$

where $\bar{p} \triangleq \lambda_{\min}(P)$.

Case b: If $1+\mu_1 < 1$ and $1+\mu_2 < 1$, then by conducting the similar analysis, one has as $s \to +\infty$ that

$$\begin{aligned} \|\eta(s)\|^2 \le& \frac{\breve{\alpha}\bar{\varpi}^2}{(1-\gamma)\bar{p}} + \frac{\bar{\upsilon}^{1-\kappa} - \bar{\upsilon}}{(1-\bar{\upsilon})\bar{p}}(\alpha_1+\alpha_2)\bar{\varpi}^2 \\ &+ \frac{\bar{\varsigma}^{2-l} - \bar{\varsigma}}{(1-\bar{\varsigma})\bar{p}}(\alpha_1+\alpha_2)\bar{\varpi}^2 < \infty. \end{aligned} \tag{31}$$

Case c: If $1+\mu_1 > 1$ and $1+\mu_2 < 1$, then by conducting the similar analysis again, one has as $s \to +\infty$ that

$$\begin{aligned} \|\eta(s)\|^2 \le& \bar{\upsilon}^{-\kappa}\frac{\breve{\alpha}\bar{\varpi}^2}{(1-\gamma)\bar{p}} + \frac{\bar{\upsilon}^{1-\kappa} - \bar{\upsilon}}{(1-\bar{\upsilon})\bar{p}}(\alpha_1+\alpha_2)\bar{\varpi}^2 \\ &+ \frac{\bar{\varsigma}^{2-l} - \bar{\varsigma}}{(1-\bar{\varsigma})\bar{p}}(\alpha_1+\alpha_2)\bar{\varpi}^2 < \infty. \end{aligned} \tag{32}$$

Thus, from (30)-(32) and Definition 1, we know that the closed-loop system (10) is ultimately bounded. The proof is now complete. ■

Remark 3: In Theorem 1, the boundedness has been analyzed for the closed-loop system (10). Particularly, the quadratic functions, which describe the scheduling behaviors of protocols, have been incorporated into the Lyapunov-like functional (LLF) to deal with the protocol-induced effects. In addition, the delay effects induced by the integral-term are also considered by constructing $V_2(k)$. Note that, when analyzing the system boundedness, the LLF is considered to be common for calculation convenience. To further reduce conservatism, the fuzzy LLF or piecewise LLF can be applied at the cost of increasing the calculation burden.

In terms of results presented in Theorem 1, the controller design issues are handled in Theorem 2.

Theorem 2: Consider the closed-loop fuzzy system (10) and the PID controller (9). Let scalars $\mu_1 > -1$ and $\mu_2 > -1$ be given. Then, the dynamics of the closed-loop system (10) is ultimately bounded if, for $i, j \in \mathbb{T}$, $d = 1, 2, \cdots, N-1$, $\epsilon \in \mathbb{L}_1$, $n \in \mathbb{L}_2$, $\bar{n} = l+1, l+2, \cdots, n_y-1$, there are positive matrices $P > 0$, $R_d > 0$, matrices K_j^P, K_j^I, K_j^D and scalars $o_{1,\bar{n}} \ge 0$, $o_{2,\bar{n}} \ge 0$, $\alpha_1 > 0$, $\alpha_2 > 0$ such that

$$\begin{bmatrix} \Lambda_n & * \\ \Theta_{i,j,n} & \bar{P}-2I \end{bmatrix} < 0 \tag{33}$$

$$\begin{bmatrix} \Lambda_n & * \\ \Theta_{i,j,n} & P-2I \end{bmatrix} < 0 \tag{34}$$

$$\begin{bmatrix} \Xi & * \\ \Gamma_{i,j,\epsilon} & P-2I \end{bmatrix} < 0 \tag{35}$$

$$\begin{bmatrix} \Xi & * \\ \Gamma_{i,j,\epsilon} & \tilde{P}-2I \end{bmatrix} < 0 \tag{36}$$

$$(1+\mu_1)^l(1+\mu_2)^\kappa < 1 \tag{37}$$

$$1 - \sum_{\bar{n}=l+1}^{n_y-1} o_{1,\bar{n}} > 0 \tag{38}$$

$$1 - \sum_{\bar{n}=l+1}^{n_y-1} o_{2,\bar{n}} > 0 \tag{39}$$

$$\bar{\mathcal{N}}_i^T\bar{\mathcal{N}}_i < P \tag{40}$$

where $\bar{\mathcal{N}}_i \triangleq \begin{bmatrix}\mathcal{N}_i & 0_{n_z \times n_\omega}\end{bmatrix}$ and other variables are defined in Theorem 1. Moreover, the minimum value of the AUB of $\|z(s)\|$ can be obtained by solving the following minimization problem:

$$\begin{cases} \min\left\{\left(\dfrac{\bar{\varsigma}^{-l}\vec{\upsilon}+\vec{\varsigma}}{1-\gamma} + \bar{\varsigma}^{1-l}\vec{\upsilon} + \tilde{\varsigma}\right)\bar{\alpha}\bar{\varpi}^2\right\} \\ \quad \text{if } 1+\mu_1 < 1 \text{ and } 1+\mu_2 > 1, \\ \min\left\{\left(\dfrac{\bar{\varsigma}^{-l}\vec{\upsilon}+\vec{\varsigma}}{1-\gamma} + \vec{\upsilon} + \tilde{\varsigma}\right)\bar{\alpha}\bar{\varpi}^2\right\} \\ \quad \text{if } 1+\mu_1 < 1 \text{ and } 1+\mu_2 < 1, \\ \min\left\{\left(\bar{\upsilon}^{-\kappa}\dfrac{\bar{\varsigma}^{-l}\vec{\upsilon}+\vec{\varsigma}}{1-\gamma} + \vec{\upsilon} + \tilde{\varsigma}\right)\bar{\alpha}\bar{\varpi}^2\right\} \\ \quad \text{if } 1+\mu_1 > 1 \text{ and } 1+\mu_2 < 1 \end{cases} \tag{41}$$

subject to constraints (33)-(40) where

$$\gamma \triangleq (1+\mu_1)^l(1+\mu_2)^\kappa, \quad \bar{\alpha} \triangleq \alpha_1+\alpha_2,$$
$$\bar{\upsilon} \triangleq \frac{1}{1+\mu_1}, \quad \bar{\varsigma} \triangleq \frac{1}{1+\mu_2},$$

This article has been accepted for publication in a future issue of this journal, but has not been fully edited. Content may change prior to final publication. Citation information: DOI10.1109/TFUZZ.2023.3282044, IEEE Transactions on Fuzzy Systems

$$\vec{\upsilon} \triangleq \frac{\bar{\upsilon}^{1-\kappa} - \bar{\upsilon}}{1-\bar{\upsilon}}, \quad \vec{\varsigma} \triangleq \frac{\bar{\varsigma}^{1-l} - \bar{\varsigma}}{1-\bar{\varsigma}}, \quad \tilde{\varsigma} \triangleq \frac{\bar{\varsigma}^{2-l} - \bar{\varsigma}}{1-\bar{\varsigma}}.$$

Proof: The Schur Complement Lemma indicates that (11) is valid if and only if the following inequality is satisfied:

$$\begin{bmatrix} \Lambda_n & * \\ \Theta_{i,j,n} & -\bar{P}^{-1} \end{bmatrix} < 0.$$

Furthermore, the fact of

$$(\bar{P} - I)\bar{P}^{-1}(\bar{P} - I) \geq 0$$

implies

$$\bar{P} - 2I \geq -\bar{P}^{-1}.$$

Thus, from the condition (33), one has that

$$\begin{bmatrix} \Lambda_n & * \\ \Theta_{i,j,n} & -\bar{P}^{-1} \end{bmatrix} \leq \begin{bmatrix} \Lambda_n & * \\ \Theta_{i,j,n} & \bar{P} - 2I \end{bmatrix} < 0.$$

By conducting the similar matrix operations, the conditions (12)-(14) in Theorem 1 are guaranteed via conditions (34)-(36), respectively.

By setting

$$o_{1,n_y} = 1 - \sum_{\bar{n}=l+1}^{n_y-1} o_{1,\bar{n}}, \quad o_{2,n_y} = 1 - \sum_{\bar{n}=l+1}^{n_y-1} o_{2,\bar{n}},$$

the conditions (16)-(17) are ensured by (38)-(39), respectively.

From the above analysis, it follows from Theorem 1 that the closed-loop system (10) is ultimately bounded. Next, by means of the condition (41), one has that

$$z^T(s)z(s) \leq \begin{bmatrix} \eta(s) \\ \omega(s) \end{bmatrix}^T P \begin{bmatrix} \eta(s) \\ \omega(s) \end{bmatrix} \leq V(s).$$

Upon taking $s \to \infty$, we can conclude from (30)-(32) that the optimization problem (41) provides the minimum value of the AUB of $\|z(s)\|$, and this completes the proof. ■

Remark 4: In Theorem 2, we have proposed a convex optimization approach to minimize the AUB under the given system decay rate. Note that the decay rate of the closed-loop system (10) is an important performance index in evaluating the control performance. To further improve the algorithm's feasibility and reduce conservatism, the AUB and the decay rate can be optimized jointly by using the well-known particle-swarm-optimization algorithm [3], [5], [7], [55].

Remark 5: Thus far, we have addressed the ultimately bounded fuzzy PID control problem for nonlinear NCSs subject to UBB noises and effects of the FRPs. First, we have modelled the transmitted outputs via a switching model and constructed a fuzzy PID controller with a concise structure. Then, in Theorem 1, sufficient conditions have been obtained to check the boundedness of the controlled system and, in Theorem 2, the desired controller gains have been derived. Note that, in Theorems 1-2, the parameters quantifying the system dynamics and the protocol effects have been adequately included.

Remark 6: In comparison to the existing literature on NCSs and fuzzy control, our paper offers the following unique contributions: 1) the investigated control problem is novel since the impacts of FRPs are analyzed for general nonlinear NCSs with UBB noises in discrete-time setting; 2) the proposed analysis method for FRPs is innovative and simplifies the design of the fuzzy PID controller; and 3) the utilized approach for boundedness analysis is more versatile, enabling the handling of various system decay rates within a unified framework.

IV. Simulation Example

This section presents a simulation example that demonstrates the effectiveness of the proposed fuzzy PID control methodology.

Consider a fuzzy system in the form of (2) with two fuzzy rules and the following parameters:

$$A_1 = \begin{bmatrix} 1 & 0 & 0.1 & 0.1 \\ 0.7 & 0.2 & 0.1 & 0.1 \\ 0.3 & 0 & 0.1 & 0 \\ 0.1 & 0.1 & 0 & 0.1 \end{bmatrix}, \quad B_1 = \begin{bmatrix} 0.5 \\ 0.1 \\ 0.5 \\ 0.1 \end{bmatrix},$$

$$A_2 = \begin{bmatrix} 1 & 0 & 0 & 0.1 \\ 0.1 & 0.2 & 0.1 & \vec{a} \\ 0.5 & 0 & 0 & 0.1 \\ 0.5 & 0 & 0 & -0.2 \end{bmatrix}, \quad B_2 = \begin{bmatrix} 0.4 \\ 0 \\ 0.6 \\ 0.1 \end{bmatrix},$$

$$C = \begin{bmatrix} 0.8 & 0 & 0.1 & 0.1 \\ 0 & 0.4 & 0.1 & 0.1 \\ 0.1 & 0.1 & 0.1 & 0 \\ 0.1 & 0 & 0.1 & 0.1 \end{bmatrix}, \quad F = \begin{bmatrix} 0.1 \\ 0 \\ 0.09 \\ 0 \end{bmatrix},$$

$$E_1 = \begin{bmatrix} 0 \\ 0.02 \\ 0 \\ 0.1 \end{bmatrix}, \quad E_2 = \begin{bmatrix} 0 \\ 0.01 \\ 0 \\ 0.05 \end{bmatrix}, \quad N_1 = \begin{bmatrix} 0.1 \\ 0.1 \\ 0.1 \\ 0.2 \end{bmatrix}^T,$$

$$N_2 = \begin{bmatrix} 0.1 & 0.1 & 0.1 & 0.2 \end{bmatrix},$$

$$x(s) = \begin{bmatrix} x_1(s) \\ x_2(s) \\ x_3(s) \\ x_4(s) \end{bmatrix}, \quad h_1(\varpi(s)) = \sin^2(x_1(s)),$$

$$y(s) = \begin{bmatrix} y_1(s) \\ y_2(s) \\ y_3(s) \\ y_4(s) \end{bmatrix}, \quad h_2(\varpi(s)) = 1 - h_1(\varpi(s)).$$

Here, the scalar $\vec{a}$ in matrix A_2 is an adjustable parameter that will be used for later comparison.

By utilizing the FRP, we set the time lengths of the static segment and dynamic segment in each communication cycle as $l = 2$ and $\kappa = 2$, respectively. It is prescribed that the first two components of $y(s)$ (i.e., $y_1(s)$ and $y_2(s)$) are scheduled by the static rules (3)-(4) in the static segment. Correspondingly, the remaining outputs $y_3(s)$ and $y_4(s)$ are scheduled by the dynamic rules (5)-(6) with $Q_3 = 1$ and $Q_4 = 2$ in the dynamic segment. The bounded external noise is assumed to be $\omega(s) = 0.5 + \mathrm{mod}(s, 2)$ which implies that $\|\omega(s)\|^2 \leq \bar{\omega}^2 = 2.25$.

The goal of this example is to design a fuzzy PID controller (9) that ensures the closed-loop system to be ultimately bounded while minimizing the upper bound of $\|z(s)\|$. Initially, we set $\vec{a} = 0.4$. The control gains obtained from Theorem 2 are then used in simulations. The results are presented in Figs. 3-7, where Figs. 3-6 depict the state evolution with and without the proposed fuzzy PID control strategy, and Fig. 7 displays the

This article has been accepted for publication in a future issue of this journal, but has not been fully edited. Content may change prior to final publication. Citation information: DOI10.1109/TFUZZ.2023.3282044, IEEE Transactions on Fuzzy Systems

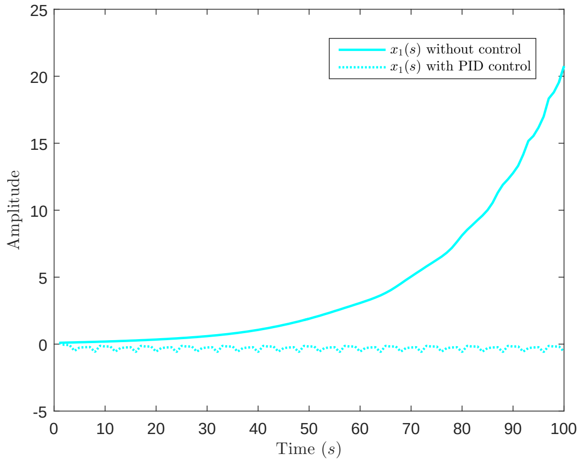

Fig. 3: The dynamic trajectory of $x_1(s)$

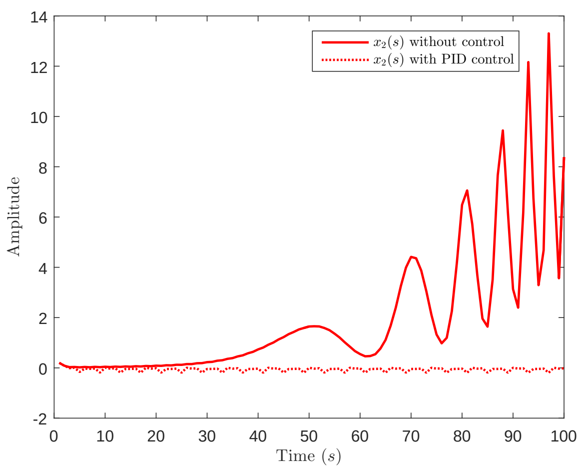

Fig. 4: The dynamic trajectory of $x_2(s)$

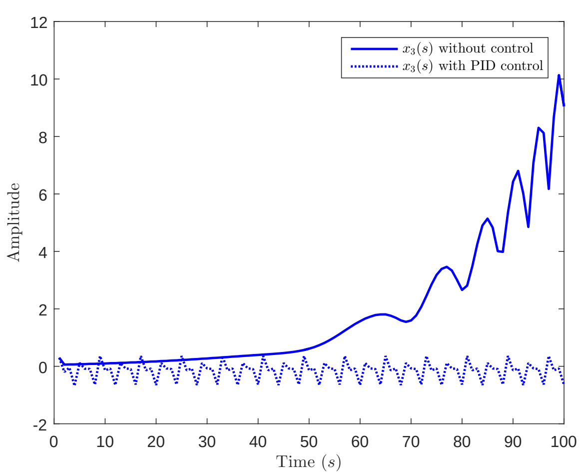

Fig. 5: The dynamic trajectory of $x_3(s)$

sensor node that has access to the network at each transmission instant.

From the simulation results, it can be observed that 1) the original open-loop system is unstable; and 2) with the

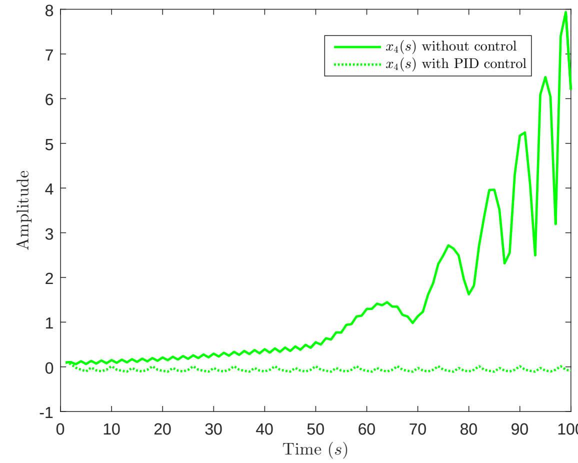

Fig. 6: The dynamic trajectory of $x_4(s)$

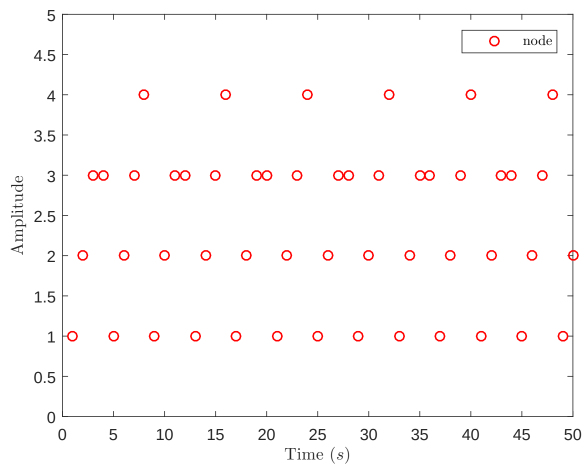

Fig. 7: The node accessing the network

proposed fuzzy PID control method, the controlled system is bounded as each component of state $x(s)$ maintains within a desired scope around the equilibrium point.

From (41), we know that the bound of the controlled signal $\|z(s)\|$ is in direct proportion to the optimized parameter $\bar{\alpha} \triangleq \alpha_1 + \alpha_2$. Thus, a smaller $\bar{\alpha}$ means a smaller bound and also a better control performance. To further demonstrate the effectiveness of the proposed fuzzy PID controller, we present a comparison with other methods in Table I and Table II. Specifically, in Table I, the parameter $\bar{\alpha}$ obtained in different system parameters $\vec{a}$ is listed. Here, the fuzzy P-type control means the traditional fuzzy static output-feedback control, which is actually a special case of our proposed fuzzy PID one (by setting $K_j^I = K_j^D = 0$). It is easy to see that the fuzzy PID controller would provide a smaller bound as compared to the traditional P-type one.

In Table II, we list the obtained x_{sum} under different UBB noises where

$$x_{\text{sum}} \triangleq \sum_{\varrho=0}^{t_f} x^T(\varrho)x(\varrho)$$

with t_f being the termination time of the simulation. Obviously, a smaller $x_{\rm sum}$ reflects a better control performance. It can be seen that our developed fuzzy PID controller is superior to the P-type one in terms of the capability of noise attenuation. Such performance improvement would benefit from the introduction of the integral term and derivative term.

To compare the results obtained based on the FRP with those derived using the TODP or RRP, we present the attained $x_{\rm sum}$ under three different communication protocols in Table III. From Table III, we can see that the FRP is indeed effective when dealing with the ultimately bounded fuzzy PID control issues. Such a good performance would benefit from the great flexibility of the FRP protocol. All simulation results show that the designed controller performs very well.

TABLE I: The Attained $\bar{\alpha}$ Using Fuzzy PID Control and Fuzzy P-type Control with Varying System Parameters

scalar $\vec{a}$	0.1	0.4	0.6	-0.1
$\bar{\alpha}$ (fuzzy P-type)	1.7565	1.8106	6.2127	2.6546
$\bar{\alpha}$ (fuzzy PID)	1.3071	1.3270	1.8342	1.6378

TABLE II: The Attained $x_{\rm sum}$ Using Fuzzy PID Control and Fuzzy P-type Control with Varying Noises

noise $\omega(s)$	$0.9\sin(s)$	$1.5\cos(s)$	1.2
$x_{\rm sum}$ (fuzzy P-type)	10.6440	29.1645	30.2807
$x_{\rm sum}$ (fuzzy PID)	5.5439	14.9701	15.6469

TABLE III: The Attained $x_{\rm sum}$ under The FRP, TODP and RRP

scalar $\vec{a}$	0.1	0.4	0.55	-0.1
$x_{\rm sum}$ (FRP)	25.2431	25.1561	25.6193	25.6970
$x_{\rm sum}$ (TODP)	26.2356	25.6593	26.0428	27.1070
$x_{\rm sum}$ (RRP)	infeasible	infeasible	infeasible	infeasible

V. Conclusion

This paper has been concerned with the fuzzy PID controller design issues for general nonlinear NCSs subject to UBB noises. We have considered that sensors send data to the remote fuzzy PID controller via a shared communication network, where the FRP has been employed to schedule network resources. The utilized FRP has been characterized by time-triggered rules and event-triggered rules which are activated alternately in the prescribed working period. By using a switching model, the measurement outputs after being transmitted have been described and then used as the controller inputs. We have established a unified framework for the boundedness analysis of the system using the switching-system theory, and designed the controller gains accordingly. The effectiveness of the proposed control method has been demonstrated through a simulation example and comparison results. The future research topics include the distributed fuzzy PID control for large-scale systems with network-induced complexities and the related applications [51], [56].

References

[1] X. Luo, H. Wu, Z. Wang, J. Wang and D. Meng, A novel approach to large-scale dynamically weighted directed network representation, *IEEE Transactions on Pattern Analysis and Machine Intelligence*, vol. 44, no. 12, pp. 9756-9773, Dec. 2022.

[2] R. Caballero-Águila, A. Hermoso-Carazo, and J. Linares-Pérez, Networked fusion estimation with multiple uncertainties and time-correlated channel noise, *Information Fusion*, vol. 54, pp. 161-171, 2020.

[3] X. Luo, Y. Yuan, S. Chen, N. Zeng and Z. Wang, Position-transitional particle swarm optimization-incorporated latent factor analysis, *IEEE Transactions on Knowledge and Data Engineering*, vol. 34, no. 8, pp. 3958-3970, Aug. 2022.

[4] D. Ciuonzo, A. Aubry, and V. Carotenuto, Rician MIMO channel- and jamming-aware decision fusion, *IEEE Transactions on Signal Processing*, vol. 65, no. 15, pp. 3866–3880, 2017.

[5] X. Guo, Z. Bi, J. Wang, S. Qin, S. Liu and L. Qi, Reinforcement learning for disassembly system optimization problems: a survey, *International Journal of Network Dynamics and Intelligence*, vol. 2, no. 1, pp. 1-14, Mar. 2023.

[6] Y. Yuan, X. Tang, W. Zhou, W. Pan, X. Li, H.-T. Zhang, H. Ding and J. Goncalves, Data driven discovery of cyber physical systems, *Nature Communications*, vol. 10, no. 1, pp. 1-9, 2019.

[7] J. Fang, W. Liu, L. Chen, S. Lauria, A. Miron and X. Liu, A survey of algorithms, applications and trends for particle swarm optimization, *International Journal of Network Dynamics and Intelligence*, vol. 2, no. 1, pp. 24-50, Mar. 2023.

[8] H. Tao, H. Tan, Q. Chen, H. Liu and J. Hu, H_∞ state estimation for memristive neural networks with randomly occurring DoS attacks, *Systems Science & Control Engineering*, vol. 10, no. 1, pp. 154-165, 2022.

[9] D. Ding, Q.-L. Han, X. Ge and J. Wang, Secure state estimation and control of cyber-physical systems: a survey, *IEEE Transactions on Systems, Man, and Cybernetics: Systems*, vol. 51, no. 1, pp. 176-190, Jan. 2021.

[10] J. Hu, C. Jia, H. Yu and H. Liu, Dynamic event-triggered state estimation for nonlinear coupled output complex networks subject to innovation constraints, *IEEE/CAA Journal of Automatica Sinica*, vol. 9, no. 5, pp. 941-944, May 2022.

[11] Z.-H. Pang, L.-Z. Fan, K. Liu and G.-P. Liu, Detection of stealthy false data injection attacks against networked control systems via active data modification, *Information Sciences*, vol. 546, pp. 192-205, 2021.

[12] Z.-H. Pang, L.-Z. Fan, Z. Dong, Q.-L. Han and G.-P. Liu, False data injection attacks against partial sensor measurements of networked control systems, *IEEE Transactions on Circuits and Systems II: Express Briefs*, vol. 69, no. 1, pp. 149-153, 2022.

[13] X. Li, S. Feng, N. Hou, R. Wang, H. Li, M. Gao and S. Li, Surface microseismic data denoising based on sparse autoencoder and Kalman filter, *Systems Science & Control Engineering*, vol. 10, no. 1, pp. 616-628, 2022.

[14] X. Ge, S. Xiao, Q.-L. Han, X.-M. Zhang and D. Ding, Dynamic event-triggered scheduling and platooning control co-design for automated vehicles over vehicular Ad-Hoc networks, *IEEE/CAA Journal of Automatica Sinica*, vol. 9, no. 1, pp. 31-46, Jan. 2022.

[15] X. Wang, Y. Sun and D. Ding, Adaptive dynamic programming for networked control systems under communication constraints: a survey of trends and techniques, *International Journal of Network Dynamics and Intelligence*, vol. 1, no. 1, pp. 85-98, Dec. 2022.

[16] V.-O. Miguel, S. S. Yuriy and G. I.-M. Oscar, Distributed unbiased FIR filtering with average consensus on measurements for WSNs, *IEEE Transactions on Industrial Informatics*, vol. 13, no. 3, pp. 1440-1447, Jun. 2017.

[17] Y. S. Shmaliy, F. Lehmann, S. Zhao and C. K. Ahn, Comparing robustness of the Kalman, H_∞, and UFIR filters, *IEEE Transactions on Signal Processing*, vol. 66, no. 13, pp. 3447–3458, 2018.

[18] Y. Ding, M. Fu, P. Luo and F. X. Wu, Network learning for biomarker discovery, *International Journal of Network Dynamics and Intelligence*, vol. 2, no. 1, pp. 51-65, Mar. 2023.

[19] J. Wu, C. Peng, H. Yang and Y. L. Wang, Recent advances in event-triggered security control of networked systems: a survey, *International Journal of Systems Science*, vol. 53, no. 12, pp. 2624-2643, 2022.

[20] F Han, J. Liu, J. Li, J. Song, M. Wang and Y. Zhang, Consensus control for multi-rate multi-agent systems with fading measurements: the dynamic event-triggered case, *Systems Science & Control Engineering*, vol. 11, no. 1, art. no. 2158959, 2023.

[21] P. Wen, X. Li, N. Hou and S. Mu, Distributed recursive fault estimation with binary encoding schemes over sensor networks, *Systems Science & Control Engineering*, vol. 10, no. 1, pp. 417-427, 2022.

[22] Y. Xu, Z. Yao, R. Lu and B. K. Ghosh, A novel fixed-time protocol for first-order consensus tracking with disturbance rejection, *IEEE Transactions on Automatic Control*, vol. 67, no. 11, pp. 6180-6186, 2022.

[23] Y. Xu, W. Lv, W. Lin, R. Lu and D. E. Quevedo, On extended state estimation for nonlinear uncertain systems with round-robin protocol, *Automatica*, vol. 138, Article 110154, 2022.
[24] D. Christmann, R. Gotzhein, S. Siegmund and F. Wirth, Realization of try-once-discard in wireless multihop networks, *IEEE Transactions on Industrial Informatics*, vol. 10, no. 1, pp. 17-26, Feb. 2014.
[25] V. Ugrinovskii and E. Fridman, A Round-Robin type protocol for distributed estimation with H_∞ consensus, *Systems and Control Letters*, vol. 69, pp. 103-110, Jul. 2014.
[26] M. C. F. Donkers, W. P. M. H. Heemels, D. Bernardini, A. Bemporad and V. Shneer, Stability analysis of stochastic networked control systems, *Automatica*, vol. 48, no. 5, pp. 917-925, May 2012.
[27] H. Chen, Y. Li, C. Liu, M. Li and H. Rao, Reliable state estimation for neural networks with TOD protocol and mixed compensation, *Neurocomputing*, vol. 492, pp. 488-495, Jul. 2022.
[28] Z. Lu and G. Guo, Control and communication scheduling co-design for networked control systems: a survey, *International Journal of Systems Science*, vol. 54, no. 1, pp. 189-203, Jan. 2023.
[29] X. Meng, Y. Chen, L. Ma and H. Liu, Protocol-based variance-constrained distributed secure filtering with measurement censoring, *International Journal of Systems Science*, vol. 53, no. 15, pp. 3322-3338, Nov. 2022.
[30] D. Tolic and S. Hirche, Stabilizing transmission intervals for nonlinear delayed networked control systems, *IEEE Transactions on Automatic Control*, vol. 62, no. 1, pp. 488-494, Jan. 2017.
[31] J. Zhang and E. Fridman, Dynamic event-triggered control of networked stochastic systems with scheduling protocols, *IEEE Transactions on Automatic Control*, vol. 66, no. 12, pp. 6139-6147, Dec. 2021.
[32] R. Makowitz and C. Temple, FlexRay-A communication network for automotive control systems, *2006 IEEE International Workshop on Factory Communication Systems*, pp. 207-212, Jun. 2006.
[33] S. Liu, Z. Wang, L. Wang and G. Wei, Recursive set-membership state estimation over a FlexRay network, *IEEE Transactions on Systems, Man, and Cybernetics: Systems*, vol. 52, no. 6, pp. 3591-3601, Jun. 2022.
[34] Y. Tang, D. Zhang, D. W. C. Ho and F. Qian, Tracking control of a class of cyber-physical systems via a FlexRay communication network, *IEEE Transactions on Cybernetics*, vol. 49, no. 4, pp. 1186-1199, Apr. 2019.
[35] W. Wang, D. Nešić and R. Postoyan, Emulation-based stabilization of networked control systems implemented on FlexRay, *Automatica*, vol. 59, pp. 73-83, Sept. 2015.
[36] W. Wang, D. Nešić and R. Postoyan, Observer design for networked control systems with FlexRay, *Automatica*, vol. 82, pp. 42-48, Aug. 2017.
[37] W. Xiong, D. W. C. Ho and S. Wen, A periodic iterative learning scheme for finite-iteration tracking of discrete networks based on FlexRay communication protocol, *Information Sciences*, vol. 548, pp. 344-356, 2021.
[38] Y. Zhao, H. Gao, S. Xu and Y. Kao, Predictor-feedback stabilization of two-input nonlinear systems with distinct and state-dependent input delays, *Automatica*, vol. 144, art. no. 110479, Oct. 2022.
[39] J. Liu, T. Yin, J. Cao, D. Yue and H. R. Karimi, Security control for T-S fuzzy systems with adaptive event-triggered mechanism and multiple cyber-attacks, *IEEE Transactions on Systems, Man, and Cybernetics: Systems*, vol. 51, no. 10, pp. 6544-6554, 2021.
[40] X.-L. Wang and G.-H. Yang, Robust filtering for fuzzy systems with bounded disturbances via premise-region-dependent event-triggered mechanisms, *IEEE Transactions on Fuzzy Systems*, vol. 30, no. 10, pp. 4093-4101, Oct. 2022.
[41] L. Chu and Y. Liu, Adaptive event-triggered control with dynamic dwell time of uncertain nonlinear systems, *International Journal of Systems Science*, vol. 54, no. 3, pp. 504-530, Feb. 2023.
[42] S. Salavati and K. Grigoriadis, Gain-scheduled output-feedback control of uncertain input-delay LPV systems with saturation via polytopic differential inclusion, *International Journal of Systems Science*, vol. 53, no. 8, pp. 1579-1599, Jun. 2022.
[43] H. K. Lam and M. Narimani, Quadratic-stability analysis of fuzzy-model-based control systems using staircase membership functions, *IEEE Transactions on Fuzzy Systems*, vol. 18, no. 1, pp. 125-137, Feb. 2010.
[44] W. Zhou, D. Luo and Z. Xu, Review of fuzzy investment research considering modelling environment and element fusion, *International Journal of Systems Science*, vol. 53, no. 9, pp. 1958-1982, 2022.
[45] Y. Wang, L. Zou, L. Ma, Z. Zhao and J. Guo, A survey on control for Takagi-Sugeno fuzzy systems subject to engineering-oriented complexities, *Systems Science & Control Engineering*, vol. 9, no. 1, pp. 334-349, 2021.
[46] X.-L. Wang and G.-H. Yang, Event-triggered controller design with varying gains for T-S fuzzy systems, *IEEE Transactions on Cybernetics*, vol. 51, no. 8, pp. 4125-4133, Aug. 2021.
[47] S. Hu, D. Yue, C. Peng, X. Xie and X. Yin, Event-triggered controller design of nonlinear discrete-time networked control systems in T-S fuzzy model, *Applied Soft Computing*, vol. 30, pp. 400-411, 2015.
[48] W. Ji, H. Zhang and J. Qiu, Fuzzy affine model-based output feedback controller design for nonlinear impulsive systems, *Communications in Nonlinear Science and Numerical Simulation*, vol. 79, art. no. 104894, Dec. 2019.
[49] Y. Wen, C. Jiao, X. Su and P. Shi, Event-triggered sliding-mode control of networked fuzzy systems with strict dissipativity, *IEEE Transactions on Fuzzy Systems*, vol. 30, no. 5, pp. 1371-1381, May 2022.
[50] Y. Wang, Z. Wang, L. Zou and H. Dong, Multiloop decentralized H_∞ fuzzy PID-like control for discrete time-delayed fuzzy systems under dynamical event-triggered schemes, *IEEE Transactions on Cybernetics*, vol. 52, no. 8, pp. 7931-7943, Aug. 2022.
[51] R. Gao and Z. Gao, Pitch control for wind turbine systems using optimization, estimation and compensation, *Renewable Energy*, vol. 91, pp. 501-515, Jun. 2016.
[52] K. Cao, X. Gao, H.-K. Lam and A. Vasilakos, H_∞ fuzzy PID control synthesis for T-S fuzzy systems, *IET Control Theory and Applications*, vol. 10, no. 6, pp. 607-616, Apr. 2016.
[53] L. Pan and X. Wang, Variable pitch control on direct-driven PMSG for offshore wind turbine using Repetitive-TS fuzzy PID control, *Renewable Energy*, vol. 159, pp. 221-237, Oct. 2020.
[54] Y. Wang, Z. Wang, L. Zou and H. Dong, Nonfragile dissipative fuzzy PID control with mixed fading measurements, *IEEE Transactions on Fuzzy Systems*, vol. 30, no. 11, pp. 5019-5033, Nov. 2022.
[55] L. Zou, Z. Wang, J. Hu and H. Dong, Ultimately bounded filtering subject to impulsive measurement outliers, *IEEE Transactions on Automatic Control*, vol. 67, no. 1, pp. 304-319, Jan. 2022.
[56] X. Liu, Z. Gao and M. Z. Q. Chen, T-S fuzzy model based fault estimation and signal compensation with application to wind turbines, *IEEE Transactions on Industrial Electronics*, vol. 64, no. 7, pp. 5678-5689, Jul. 2017.

Yezheng Wang received the B.Eng. degree in automation from the Qilu University of Technology, Jinan, China, in 2017. He is currently pursuing the Ph.D. degree from the College of Electrical Engineering and Automation, Shandong University of Science and Technology, Qingdao, China. Since February 2023, he has been a Visiting Ph.D. Student with the Department of Computer Science, Brunel University London, Uxbridge, U.K.

His current research interests include the control and filtering for T-S fuzzy system.

Mr. Wang is a very active reviewer for many international journals.

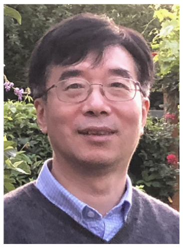

Zidong Wang (SM'03-F'14) received the B.Sc. degree in mathematics in 1986 from Suzhou University, Suzhou, China, and the M.Sc. degree in applied mathematics in 1990 and the Ph.D. degree in electrical engineering in 1994, both from Nanjing University of Science and Technology, Nanjing, China.

He is currently a Professor of Dynamical Systems and Computing in the Department of Computer Science, Brunel University London, U.K. From 1990 to 2002, he held teaching and research appointments in universities in China, Germany and the U.K. Prof. Wang's research interests include dynamical systems, signal processing, bioinformatics, control theory and applications. He has published more than 700 papers in international journals. He is a holder of the Alexander von Humboldt Research Fellowship of Germany, the JSPS Research Fellowship of Japan, William Mong Visiting Research Fellowship of Hong Kong.

Prof. Wang serves (or has served) as the Editor-in-Chief for *International Journal of Systems Science*, the Editor-in-Chief for *Neurocomputing*, the Editor-in-Chief for *Systems Science & Control Engineering*, and an Associate Editor for 12 international journals including IEEE Transactions on Automatic Control, IEEE Transactions on Control Systems Technology, IEEE Transactions on Neural Networks, IEEE Transactions on Signal Processing, and IEEE Transactions on Systems, Man, and Cybernetics-Part C. He is a Member of the Academia Europaea, a Member of the European Academy of Sciences and Arts, an Academician of the International Academy for Systems and Cybernetic Sciences, a Fellow of the IEEE, a Fellow of the Royal Statistical Society and a member of program committee for many international conferences.

Lei Zou received the Ph.D. degree in control science and engineering in 2016 from Harbin Institute of Technology, Harbin, China.

He is currently a Professor with the College of Information Science and Technology, Donghua University, Shanghai, China. From October 2013 to October 2015, he was a Visiting Ph.D. Student with the Department of Computer Science, Brunel University London, Uxbridge, U.K. His research interests include control and filtering of networked systems, moving-horizon estimation, state estimation subject to outliers, and secure state estimation.

Prof. Zou serves (or has served) as an Associate Editor for *IEEE/CAA Journal of Automatica Sinica*, *Neurocomputing*, *International Journal of Systems Science*, and *International Journal of Control, Automation and Systems*, a Senior Member of *IEEE*, a Member of *Chinese Association of Automation*, a Regular Reviewer of *Mathematical Reviews*, and a very active reviewer for many international journals.

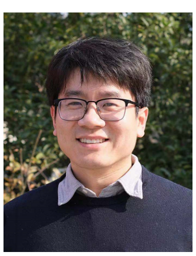

Lifeng Ma received the B.Sc. degree in Automation from Jiangsu University, Zhenjiang, China, in 2004 and the Ph.D. degree in Control Science and Engineering from Nanjing University of Science and Technology, Nanjing, China, in 2010. From August 2008 to February 2009, he was a Visiting Ph.D. Student in the Department of Information Systems and Computing, Brunel University London, U.K. From January 2010 to April 2010 and May 2011 to September 2011, he was a Research Associate in the Department of Mechanical Engineering, the University of Hong Kong. From March 2015 to February 2017, he was a Visiting Research Fellow at the King's College London, U.K.

He is currently a Professor in the School of Automation, Nanjing University of Science and Technology, Nanjing, China. His current research interests include control and signal processing, machine learning and deep learning. He has published more than 50 papers in refereed international journals. He serves as an editor for *Neurocomputing* and *International Journal of Systems Science*.

Hongli Dong received the Ph.D. degree in control science and engineering from the Harbin Institute of Technology, Harbin, China, in 2012.

From 2009 to 2010, she was a Research Assistant with the Department of Applied Mathematics, City University of Hong Kong, Hong Kong. From 2010 to 2011, she was a Research Assistant with the Department of Mechanical Engineering, The University of Hong Kong, Hong Kong. From 2011 to 2012, she was a Visiting Scholar with the Department of Information Systems and Computing, Brunel University London, London, U.K. From 2012 to 2014, she was an Alexander von Humboldt Research Fellow with the University of Duisburg–Essen, Duisburg, Germany. She is currently a Professor with the Artificial Intelligence Energy Research Institute, Northeast Petroleum University, Daqing, China. She is also the Director of the Heilongjiang Provincial Key Laboratory of Networking and Intelligent Control, Daqing, China. Her current research interests include robust control and networked control systems.

Dr. Dong is a very active reviewer for many international journals.